

# Extended Lattice Gas Interactions of Cu on Cu(111) and Cu(001): Ab-Initio Evaluation and Implications

T. J. Stasevich\* and T. L. Einstein†

*Department of Physics, University of Maryland, College Park, Maryland 20742-4111, USA*

Sergey Stolbov

*Department of Physics, Cardwell Hall, Kansas State University, Manhattan, Kansas 66506, USA*

(Dated: March 21, 2006)

We present ab-initio calculations of a variety of different lattice-gas interaction energies between Cu adatoms on Cu(001) and Cu(111). We find the next-nearest-neighbor (NNN) interactions to be negligible on Cu(111), explaining the success of the nearest-neighbor (NN) Ising model when describing the Cu(111) step stiffness. On Cu(001), however, we find that NNN interactions are roughly (1/7) the attractive NN interaction strength. On both surfaces, we find longer-range pair interactions to be small, although there are relatively large trio interactions. On Cu(111) these include two orientation dependent trios composed of adatoms forming a NN-triangle. We calculate the interaction energies of these trios and show that they can account for the difference in formation energies between A- and B-steps. On Cu(001), we find the trio interaction composed of adatoms forming a NN-isosceles right triangle to be quite large and repulsive. This contradicts our theoretical expectations, which suggest the interaction should be attractive to account for the Cu(001) step stiffness. Finally, by calculating the bulk energy per atom in multiple ways, we show our calculations are self-consistent.

PACS numbers: 68.35.Md 71.15.Nc 05.70.Np 81.10.Aj

## I. INTRODUCTION

Lattice-gas models provide a powerful and convenient route to explore how microscopic energies influence the statistical mechanics of mesoscopic structures on crystalline surfaces. Such models underlie most Monte Carlo (and transfer matrix) simulations. They assume that overlayer atoms (or other adsorbed units) sit at particular high-symmetry sites of the substrate, an intrinsic assumption of epitaxial growth, for example. The parameters of the model are then the interaction energies between such atoms and/or the barriers associated with hops between the high-symmetry positions.

The use of lattice-gas models proceeds in two generic ways. In the first, one posits a few energies that are likely to dominate the physics of interest and then computes with Monte Carlo simulations the desired equilibrium or dynamic properties, deriving thereby the values of these energies from fits<sup>1</sup>. The dangers of this approach are: a) the properties of interest may be relatively insensitive to the specific interactions and b) there may be other interactions that are non-negligible, so that the deduced energies are effective rather than actual.

The second approach<sup>2-5</sup> begins by actually computing the (many) energies of importance, a task that is now possible with efficient density-functional-theory packages such as VASP (the Vienna Ab-initio Simulation Package).<sup>6</sup> This process can be used to compute interaction energies between relatively distant neighbors. One should also compute multi-atom interactions, which can also be significant.<sup>7,8</sup> This approach is appealing because the calculated interaction energies can be self-consistently checked for completeness, thereby diminish-

ing the risk discussed in (b) above. Assuming that one has sufficient computational power to compute all the interactions that contribute at the level of the desired precision, there is still the danger that the interactions depend sensitively on the local environment, making a simple lattice gas description inadequate.

These caveats notwithstanding, lattice gas models have been extensively used in the realm of surface physics to describe such diverse phenomena as phase transitions, concentration-dependent diffusion, and growth. We have recently used such a model to compute the orientation dependence of step stiffness—the inertial parameter for steps in the step continuum model<sup>9</sup>—for the (001) and (111) faces of Cu.<sup>10,11</sup> This work illustrates both successes and some shortcomings of using a lattice-gas model with just nearest-neighbor (NN) interactions: whereas the step stiffness on Cu(111) is well described by NN interactions alone, the step stiffness on Cu(001) requires the inclusion of next-nearest neighbor (NNN) and perhaps even trio interactions. In this case, a firm understanding of the adatom interactions would be an ideal way to construct an appropriate theory.

With this goal in mind, we have performed ab-initio calculations to determine the strengths of interactions between Cu adatoms on Cu(001) and Cu(111). For these systems we have tested the applicability of a lattice-gas model and have determined which interactions are essential and which can be ignored.

Fig. 1 shows a summary of the calculated interactions between Cu adatoms on Cu(111); the corresponding interactions on Cu(001) are analogous. The first row shows the pairwise interactions of interest. Besides NN interactions (of energy  $E_1$ ), we have also considered  $n^{\text{th}}$  nearest-

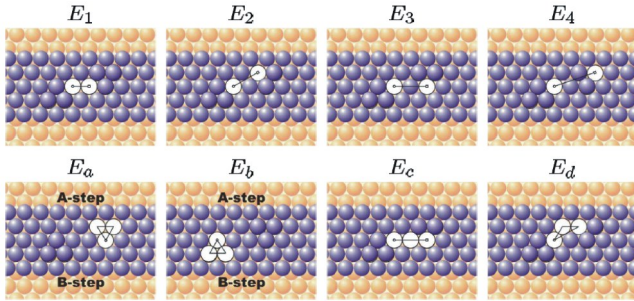


FIG. 1: (Color online) Interactions of interest (only shown for Cu(111); the interactions on Cu(001) are analogous). Dark blue spheres represent adatoms, lighter orange spheres represent substrate atoms, and white spheres represent adatoms involved in the interactions of interest. Pair interactions are shown in the top row, and trio interactions are shown in the bottom row.

neighbor interactions (of energy  $E_n$ ) out to  $n=4$ . Based on our previous work,<sup>10,11</sup> as described above, we expect NNN interactions to be negligible on Cu(111), but significant on Cu(001).

The second row of Fig. 1 shows the trio-interactions of interest. These interactions are the non-pairwise part of the interaction among three nearby adatoms.<sup>7,8</sup> These include the trios ( $E_{a/b}$ ) for three NN adatoms forming an equilateral triangle (for which no Cu(001) counterparts exist), the trio ( $E_c$ ) for three collinear adatoms, and the trio ( $E_d$ ) for three adatoms forming a NN-isosceles triangle with apex angle  $90^\circ$  on Cu(001) and  $120^\circ$  on Cu(111) (the ‘d’ stands for ‘dent’). Based on our previous work,<sup>10</sup> we expect  $E_d$  to affect the step stiffness on Cu(001) in the same way as  $E_2$  (so that the effective NNN interaction is  $E_2 + E_d$ ).

As illustrated in the two lower-left sub-figures of Fig. 1, when one includes the substrate layer upon which adatoms are adsorbed, the 6-fold symmetry of the adsorption layer is reduced to 3-fold. One should then, at least in principle, distinguish between the trio interactions  $E_a$  and  $E_b$ . Whereas  $E_a$  triangles are made from A-microfacets,  $E_b$  triangles are made from B-microfacets. As we noted earlier,<sup>11</sup> the difference between  $E_a$  and  $E_b$  provides the simplest way to account for the difference between energies of A- and B-steps within a lattice gas framework.

The remainder of this paper is divided into three sections and an Appendix. In the next section we describe the details of our calculations. In Section III we present and discuss our results and the implications. Finally, we summarize and offer concluding remarks in Section IV. The attached Appendix provides details related to the error analysis of our computations.

## II. METHOD

To accurately gauge the relative size of the Cu adatom-interactions of interest within the framework of density functional theory,<sup>12,13</sup> we used VASP,<sup>6</sup> together with the supplied Cu ultrasoft-pseudopotential (with a basis energy cut-off of 17.2 Ry), and the Perdew-Wang ’91 generalized gradient approximation<sup>14</sup> (GGA). To speed up electronic relaxation, we used the method of Methfessel and Paxton<sup>15</sup> with a width of 0.2 eV.

We modeled the surfaces of Cu(001) and Cu(111) by constructing two large supercells for each surface, one containing up to  $(14 \times 3 \times 2)$  atoms, the other containing up to  $(14 \times 4 \times 2)$  atoms; we refer to these, respectively, as  $(3 \times 2)$  and  $(4 \times 2)$ . Using the  $(3 \times 2)$  cell, fourth-neighbor pair interactions and beyond were assumed to be negligible and therefore ignored, whereas using the  $(4 \times 2)$  cell, for self-consistency, fourth-neighbor pair interactions were included (and ultimately verified to be negligible). To assure energy convergence to within a few meV, we sampled the Cu(111)  $(4 \times 2)$  supercell using a  $(6 \times 12 \times 1)$  mesh of  $\mathbf{k}$ -points, and the Cu(001)  $(4 \times 2)$  supercell using a  $(5 \times 10 \times 1)$  mesh. A similar density of  $\mathbf{k}$ -points was used for the  $(3 \times 2)$  cells. (Because we never directly compared energies between cells, maintaining the same density of  $\mathbf{k}$ -points between cells was irrelevant.)

We began all calculations by filling the first seven layers of the supercell, thereby producing—when periodically repeated in the three orthonormal symmetry directions—a series of seven-layer-thick, parallel slabs buffered by seven layers of vacuum. Here, as in all calculations, the slab lattice parameter was fixed at 3.64 Å—the value obtained from a bulk GGA calculation for a  $(1 \times 1 \times 1)$  supercell sampled using an  $(11 \times 11 \times 11)$  mesh of  $\mathbf{k}$ -points. We then computed the slab energy in two ways: first with relaxation constrained to be normal to the surface, and second with full relaxation. In both cases, we held the inner three layers of atoms fixed at their calculated bulk positions, while the outer-layer atoms relaxed until the net force on them was less than 0.01 eV/Å.

Next we placed adatoms on the top and bottom of the slab. The seven-layer slab is (just) thick enough that through-substrate interactions<sup>16</sup> between the adatoms are insignificant, causing uncertainties no greater than 30meV. (See Appendix for details.) An alternative would be to put adatoms on just one side of the slab,<sup>4,17,18</sup> which would allow thinner slabs to be used for the substrate. (Since we are considering homoepitaxy, presumably there would be minimal charge-transfer effects requiring correction,<sup>16</sup>) We then recomputed the total energy in the same ways as before, allowing for both full and constrained (perpendicular to the surface) relaxation. We repeated this procedure for a variety of adatom arrangements. This allowed us to construct a set of independent equations that we could solve to obtain the various interaction energies of interest.

To illustrate our technique, Fig. 2 depicts all Cu(001) calculations. The figure shows the top (001) surface of

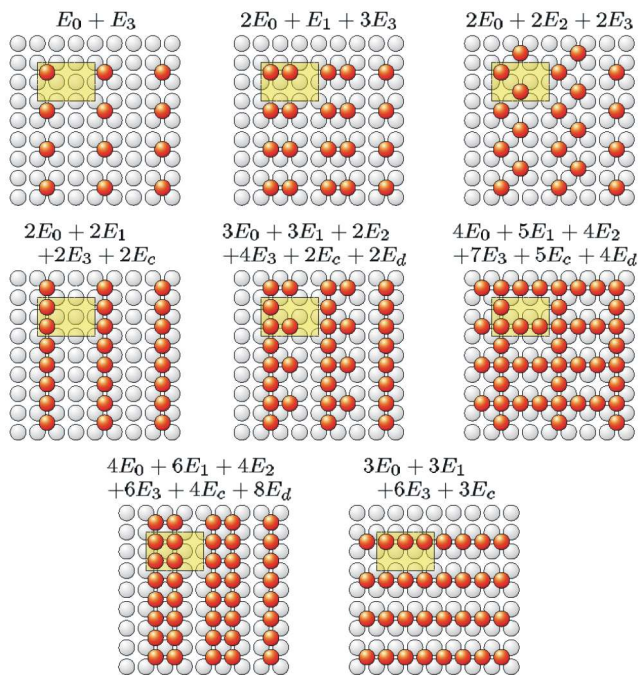


FIG. 2: (Color online) A summary of calculations performed for Cu(001). Each sub-figure corresponds to a different arrangement of adatoms (dark-orange spheres) on the substrate (light-gray spheres) with total energy given by a different linear combination of adatom interaction energies. When taken together, any six equations can be solved to determine the six energies of interest.

the aforementioned seven-layer slab (the [yellow] boxed region representing the top of the supercell); the lighter gray spheres represent surface atoms while the darker [orange] spheres represent adatoms. Although the bottom of the cell is not shown, we constructed it to be identical to the top.

The upper-left subfigure shows the arrangement of adatoms used in our first calculation. For this arrangement, the top and bottom surface of each supercell contains one adatom, so that the energy per supercell — after subtracting off the slab energy — is  $E_0 + E_3$ , where  $E_0$  is the energy of introducing and adsorbing an atom on a clean substrate. Interactions beyond third neighbors are neglected, but interactions between supercell images up to third-neighbors are scrupulously included.

The top-middle subfigure shows the arrangement of adatoms used in our second calculation. Here, the top and bottom of each supercell contains two NN adatoms. Summing over all intra- and inter-supercell interactions as before, the energy of this configuration (again minus the slab energy) is  $2E_0 + E_1 + 3E_3$ .

Continuing in this way, we generated six more equations with the introduction of just three more unknowns:  $E_2$ ,  $E_c$  and  $E_d$ . In total, then, we were left with eight independent equations, of which we could choose any six to solve simultaneously for the six interaction energies of interest. By comparing solutions from different sets of

equations, we could self-consistently check our energies and also roughly estimate—by noting the variation in values—the error in the calculations. (See the Appendix for more details.)

In much the same way—as illustrated in Fig. 3—we calculated adatom interaction energies for the Cu(111) (3x2) cell, the only noteworthy difference being the evaluation of the NN-trio interaction energies,  $E_{a/b}$ . Instead of eight, there were now ten independent equations (only nine are shown in Fig. 3—the missing configuration is identical to the middle subfigure with up-pointing triangles instead of down-pointing, so that  $E_a$  is replaced with  $E_b$ ), of which we could choose any eight to solve for the eight interaction energies of interest.

Finally, the entire process was repeated for the (4x2) cells. Although most of the configurations remained unchanged, the inclusion of  $E_4$  required a few additions and minor modifications in order to obtain the proper number of independent equations.

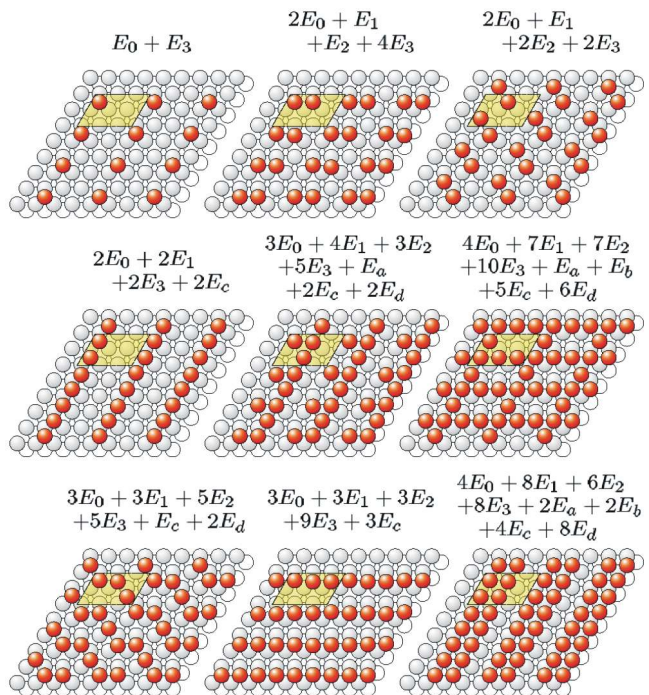


FIG. 3: (Color online) A summary of calculations performed for Cu(111). As in Fig. 2, each sub-figure corresponds to a different arrangement of adatoms (dark-orange spheres) on the substrate (light-gray spheres) with total energy given by a different linear combination of interaction energies. Here, however, because the triangle trio interactions depend on orientation, there is an interaction energy  $E_a$  for down-pointing triangles and  $E_b$  for up-pointing triangles. When taken together, any eight equations can be solved to determine the eight energies of interest. (Note that the up-pointing trio arrangement is not shown above.)

### III. RESULTS AND DISCUSSION

The results of our calculations are listed in Table I. Only data for full relaxation are shown because data for constrained relaxation do not differ in any significant way: Specifically, data for the fully relaxed Cu(001) (3x2) cell differed from their vertically relaxed counterparts by no more than 13 meV, and often by less than 5 meV (the differences typically in proportion to the size of the interaction). Provided the system is not in a metastable state, this observation corroborates the description of Cu surface energetics using a lattice gas model, where one assumes atoms sit at preferential, high-symmetry positions. In other words, while relaxation from these preferred positions inevitably occurs, the amount of relaxation negligibly changes the various interaction energies of importance. We therefore only require a finite number of ‘typical’ or ‘average’ interactions to fully describe the system, making a lattice-gas model appropriate.<sup>19</sup>

Besides the interaction energies discussed earlier, estimates for  $E_0$ , the energy of introducing and adsorbing an atom on a clean substrate, and  $E_s$ , the surface energy per atom, on both Cu(001) and Cu(111) are included ( $E_s$  was calculated by comparing slab energies of varying thickness, as discussed in the literature.<sup>20</sup>) The surface energies compare well with previous results; in particular, Spišák<sup>21</sup> found the surface energy of Cu(001) to be 606 meV/atom, while Wang *et al.*<sup>22</sup> found it to be 582 meV/atom. Our estimate of 600 meV/atom agrees with both. Similarly, Wang<sup>22</sup> estimated the surface energy of Cu(111) to be 462 meV/atom, in nearly exact agreement with our result.

The accuracy of our calculations is further confirmed by the excellent overall agreement between results using the (3x2) and (4x2) cells, where energies would typically differ because of a difference in  $\mathbf{k}$ -point sampling. Furthermore, the agreement between cells suggests that longer-range interactions are negligible: a different cell size means that adatoms are arranged in a different geometry, which implies that a different number of long-range interactions are ignored. If the long-range interactions are significant, the calculated energies should differ from one cell size to the other. Because they do not differ, the long-range interactions are most likely negligible (unless they happen to cancel each other), confirming our original assumption.

We begin the discussion of our computed lattice-gas energies with the pair interactions. We find  $E_1$  to be the most attractive on both surfaces. This result could be anticipated, since stable adatom islands are often experimentally observed on these surfaces. Furthermore, the strength of the interaction is stronger on Cu(001) than on Cu(111). This result is consistent not only with bond-order-bond-strength arguments<sup>23</sup> applied to the direct part of the interaction (adatoms have six nearest neighbors on Cu(111) compared to four on Cu(001)), but also with the general result for the semiempirical embedded atom method (EAM) formalism that the leading

$E(\text{meV})$	Cu(001)		Cu(111)	
	(3x2)	(4x2)	(3x2)	(4x2)
$E_s$	600	600	462	465
$E_0$	-3149±16	-3146±14	-2922±15	-2920±12
$E_1$	-332±16	-335±12	-314±19	-323±11
$E_2$	-47±9	-43±6	4±12	1±12
$E_3$	-3±9	-13±8	5±6	3±3
$E_4$	–	2±4	–	-1±3
$E_a$	–	–	117±23	101±23
$E_b$	–	–	83±23	79±23
$E_c$	-14±11	-16±18	-22±11	-25±13
$E_d$	51±11	54±11	-11±11	9±23

TABLE I: Calculated adatom interaction energies (in meV) on Cu(001) and Cu(111). Here  $E_i$  ( $i=1,2,3,4$ ) is the  $i^{\text{th}}$  neighbor interaction,  $E_i x$  ( $x=a, b, c, d$ ) are trio interactions as depicted in Fig. 1 (with Ed corresponding to a right isosceles triangle for the (001) substrate),  $E_0$  is the energy of introducing an adsorbed adatom on an empty substrate, and  $E_s$  is the surface energy per atom, with corresponding units of meV/atom. See Appendix for a discussion of error bars.

contribution to the indirect (substrate-mediated) part of the interaction is attractive (negative) and proportional to the number of shared NN substrate atoms: two for Cu(001) and one for Cu(111).<sup>8</sup>

Moving on to higher-order interactions, we find  $E_2$  to be a negligible fraction of  $E_1$  on Cu(111), whereas it is a significant  $(1/7)E_1$  on Cu(001). As before, this is consistent with EAM findings; after all, NNN share no substrate atoms on Cu(111), while they share a single substrate atom on Cu(001). Furthermore, this explains why the NN lattice-gas model does not adequately describe the orientation dependence of the step stiffness on Cu(001), but successfully describes the same property on Cu(111).<sup>10,11</sup> In essence, whereas NNN interactions can be ignored in the latter case, they cannot be in the former.

Rounding out our analysis of the pair interactions, we find  $E_3$  and  $E_4$  to be very small on both surfaces, consistent with the agreement between the (3x2) and (4x2) results. (Recall that we did not include  $E_4$  in the (3x2) calculations. Earlier calculations<sup>2</sup> also found  $E_3$  to be essentially negligible on (111).) Notice, however, that even though these interactions are quite small, the general trend  $|E_n| > |E_{n+1}|$  is predominantly preserved.

In the only systematic semiempirical investigation of Cu/Cu(001) (or, for that matter, Cu/Cu(111)) pair interactions of which we are aware, Levanov *et al.*<sup>24</sup> found values in remarkably decent agreement with ours:  $E_1 = -0.32$  eV,  $E_2 = -0.04$  eV, and  $E_3 = +0.01$  eV.

We next consider the trio interactions, beginning with the observation that the largest trio interactions  $E_a$  and  $E_b$  are equilateral triangular in geometry and repulsive in nature, a result which agrees with a similar study on Ag(111)<sup>4</sup>. The collinear trio,  $E_c$ , on the other hand, is

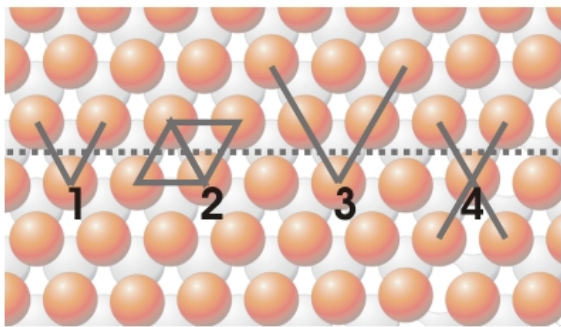


FIG. 4: (Color Online) When the atoms (dark orange spheres) are separated along the dashed line to create an A- and B-step pair, a number of bonds are broken. In the process, atom 1 shows that two NN bonds ( $E_1$ ) are broken per atom, atom 2 shows that two NN trio bonds ( $E_{a/b}$ ) are broken per atom, and atoms 3 and 4 show that four collinear trio bonds ( $E_c$ ) are broken per atom.

attractive and not as significant, being of moderate to small size on both surfaces.

As we discussed earlier, the difference between  $E_a$  and  $E_b$  can account for the difference in the formation energies of A- and B-steps. Here we find  $E_b \lesssim E_a$ , suggesting B steps are marginally more favorable than A-steps. If we further assume, as our calculations suggest, that only  $E_1$ ,  $E_{a/b}$ , and  $E_c$  are non-negligible interactions (specifically, interactions having a magnitude greater than 5 meV when averaged between the two cell sizes), then from bond breaking arguments, the formation energies per atom of A- and B-steps,  $E_A$  and  $E_B$ , can be written:

$$E_A = -E_1 - \frac{1}{3}E_a - \frac{2}{3}E_b - 2E_c \quad (1)$$

$$E_B = -E_1 - \frac{2}{3}E_a - \frac{1}{3}E_b - 2E_c. \quad (2)$$

Notice that  $E_A + E_B = -2E_1 - E_a - E_b - 4E_c$ , that is, to form an A- and B-step pair, two NN bonds must be broken per atom, along with six trio bonds: one  $E_a$ , one  $E_b$ , and four  $E_c$  (see Fig. (4)). Combining Eqs. (1) and (2) with our results (where we average between the (3x2) and (4x2) cell calculations), we find  $E_A \simeq 277 \pm 23$  meV/atom, while  $E_B \simeq 267 \pm 23$  meV/atom, so their ratio is  $1.04 \pm 0.12$ . These estimates agree with previous results of 0.27 and 0.26 eV, respectively, by Feibelman using a much larger cell.<sup>25</sup> Within error bars, these estimates are also in accord with recent semiempirical EAM calculations that found the two values to be 263 and 265 meV,<sup>26</sup> with a ratio consistent with earlier EAM deductions.<sup>27</sup> All these calculations are consistent with measurements by Giesen,<sup>28</sup> who reports ratios of 1.011 and 0.98; controversy remains as to whether the ratio is marginally larger or smaller than unity. Thus, as a whole, this simple lattice gas model appears to be quite successful.

We now consider the calculated strengths of the remaining interactions  $E_d$ . Although they are relatively small on Cu(111), they are fairly sizable and repulsive on Cu(001). Based on our previous theory,<sup>10</sup> we expect  $E_d$  to renormalize  $E_2$  on Cu(001) so that  $E_2 + E_d \simeq 1/4 E_1$ . Surprisingly, though, we find  $E_2 + E_d \simeq 0$ ! Thus, whereas the inclusion of our calculated attractive  $E_2$  interactions help explain the discrepancy between theory and experiment with regards to the orientation dependence of step-stiffness, the inclusion of our calculated repulsive  $E_d$  interactions magnify the discrepancy.

Beyond the tabulated interactions, we also estimated the size of more distant neighbor triangular trio interactions on Cu(001) (interactions we could easily include because we calculated the energies of more configurations than unknowns for self-consistency). In particular, we looked at the isosceles triangle trio composed of two NNN legs and a third-nearest-neighbor hypotenuse and the right-triangle trio with one NN leg and one third-nearest-neighbor leg. In both cases, the interaction strengths were negligibly small, of order 5 meV.

Finally, we can obtain the bulk energy per atom  $E_{bu}$  from the calculated lattice-gas interaction energies. To do so, we note that an extra layer of atoms in the slab can be thought of as the addition of a bulk layer or an adsorbed layer. In the first case, the additional energy is just the number of atoms  $N$  in the new layer times  $E_{bu}$ . In the second case, the energy is  $N$  times  $E_0$  plus the sum of all significant lateral lattice-gas interaction energies (again, interactions having a magnitude greater than 5 meV when averaged between the two cells.) Equating these and dividing by  $N$  gives

$$E_{bu} \simeq E_0 + 2E_1 + 2E_2 + 2E_3 + 2E_c + 4E_d, \quad (3)$$

for Cu(001) and

$$E_{bu} \simeq E_0 + 3E_1 + E_a + E_b + 3E_c, \quad (4)$$

for Cu(111). While there are many other longer-range and multiatom interactions, they are expected not only to become very small but also to tend to cancel each other.<sup>8</sup> Thus, how well these estimates of  $E_{bu}$  agree provides a practicable gauge of self-consistency. Not only are the right-hand-sides of both equations independently equal, but they are independently equal to  $E_{bu}$ : a quantity that was, itself, independently calculated when we determined the slab lattice parameter (using a (1x1x1) supercell sampled with (11x11x11)  $\mathbf{k}$ -points). There we found  $E_{bu} = -3763$  meV/atom. This agrees quite well (considering the error) with Eqs. (3) and (4), which give, respectively,  $E_{bu} = -3741 \pm 48$  meV/atom and  $E_{bu} = -3760 \pm 35$  meV/atom (averaged between (3x2) and (4x2) cells). The self-consistency of these calculations corroborates the general success of the lattice-gas model.

#### IV. CONCLUSIONS

We have calculated from first principles a variety of different Cu adatom interaction energies on both Cu(001) and Cu(111). For the most part, our calculations have confirmed our expectations. First, we have shown that the computed interaction energies are robust with respect to small, lateral relaxations of the adatoms: an important requirement for a successful lattice-gas theory. Second, we find  $E_2$  interactions to be negligible on Cu(111) but significant on Cu(001), explaining why the NN lattice gas model successfully describes the orientation dependence of the Cu(111) step stiffness, but fails for Cu(001). Third, we have used our calculated lattice-gas interaction energies to determine the formation energies of Cu(111) A- and B-steps. The resulting estimates for the formation energies agree well with the literature. Fourth, we have shown that for Cu on Cu, as expected, adatom pair interactions drop off quickly with distance, and only the geometrically smallest trio interactions are relevant. Finally, we have shown that our calculations for the lattice-gas interaction energies are self-consistent and, when taken together, can be used to accurately find the bulk energy per atom  $E_{bu}$ .

Considering these successes, the the relatively large value of  $E_d$  on Cu(001) was unexpected. When this repulsive interaction is included in a theory of the orientation dependence of step stiffness, it renormalizes  $E_2$  to zero (since the right-triangle trio produces an effective value of  $E_2$  that is  $E_2 + E_d$ , as argued in Ref. 10). To the extent that this value of  $E_d$  is reliable,<sup>29</sup> there remains a discrepancy between the NN-Ising theory and experiment a mystery. One possible explanation is the existence of other significant many-body interactions that make the calculated  $E_d$  effective rather than actual. It is interesting to note, for example, that  $E_{bu}$  is slightly underestimated by the Cu(001) lattice-gas interactions, suggestive of a too repulsive  $E_d$ . Considering the overall self-consistency of our results, however, such many-body interactions are most likely negligible. Another possible explanation we are currently exploring suggests that calculated trio interaction energies can vary significantly between LDA and GGA calculations, whereas pair interactions remain unchanged. We are currently looking further into this issue for Pt on Pt systems,<sup>29</sup> where more asymmetry between A- and B-steps exists, and where results for kink-formation energies (which are directly related to  $E_a$  and  $E_b$ ) are known to be worse for GGA than for LDA.<sup>25,30</sup>

In closing, we believe first-principle calculations such as the ones described here will prove useful in determining the limits of lattice gas models applied to all sorts of systems. Although we began with strong expectations based on previous theory and experiment, the consistency of our results shows that the problem can be worked in reverse; that is, based on first-principle calculations, we can determine what kinds of interactions need to be included in the system to make a successful

lattice-gas model.

#### Acknowledgments

Work supported primarily by the University of Maryland NSF-MRSEC, grant DMR 05-20471, with partial support from DOE Grant DE-FG02-03ER46058 (S.S.) and from NSF Grant EEC-0085604, which supported collaborations with Talat Rahman and Kristen Fichthorn, whom we thank for helpful interactions contributing to this paper. Computations were supported by the National Computational Science Alliance under NSF DMR 030054 and were performed on the IBM p690 at the University of Illinois. We thank Rajesh Sathiyarayanan for assistance in the final stages of the calculations and Hailu Gebremariam for frequent discussions.

#### APPENDIX

In Table I energies are listed with error bars. Here, the source of error was predominantly due to interactions between adatoms through the substrate. Whereas increasing the slab thickness would have reduced this error, the required computational time would have increased significantly.<sup>16</sup> Instead, we effectively reduced error by averaging results over a set of self-consistent calculations. More precisely, we calculated the energies of more adatom arrangements than were necessary to solve for the interaction energies of interest. By choosing different sets of arrangements to solve for the same interaction energies, we could self-consistently check our results while at the same time estimate error. Typically, interaction energies changed little from one set of arrangements to another, though differences could be on the order of 10-30 meV. We therefore assumed each total-energy calculation carried an error of 30 meV. With this assumption, the propagation of error was easily calculated.

As an example, using the first six adatom arrangements shown in Fig. 2, we could simultaneously solve the corresponding six equations for the six interaction energies of interest. Assuming the six configurations correspond to energies  $\mathcal{E}_i \pm 30$  meV,  $i=1,2,\dots,6$ , then, for example,  $E_1$  is

$$E_1 = \frac{1}{12}(5\mathcal{E}_S - 10\mathcal{E}_1 + 2\mathcal{E}_2 + \mathcal{E}_4 + 4\mathcal{E}_5 + 2\mathcal{E}_6), \quad (5)$$

where  $\mathcal{E}_S \pm 30$  meV corresponds to the energy of the slab without any adatoms. The error in this estimate is therefore

$$\begin{aligned} \Delta E_1 &= \frac{1}{12} \sqrt{5^2 + 10^2 + 2^2 + 1 + 4^2 + 2^2} \Delta E & (6) \\ &= 1.02 \Delta E, & (7) \end{aligned}$$

where  $\Delta E \equiv 30$  meV. Similarly, solving for  $E_2$  gives

$$E_2 = \frac{1}{4}(\mathcal{E}_S - 2\mathcal{E}_1 + \mathcal{E}_4), \quad (8)$$

with corresponding error

$$\Delta E_2 = \frac{1}{4} \sqrt{1 + 2^2 + 1} \Delta E \quad (9)$$

$$= 0.61 \Delta E. \quad (10)$$

Continuing in this way, we estimated the error of all the calculated interaction energies of interest. We then repeated the process for different sets of six arrangements of adatoms. Of course, different sets yield different errors. By averaging over results from sets of arrangements with the least error (which inevitably agreed the most), we reduced the error even further.

One potential danger of using this method of error analysis is the presence of systematic error that doesn't

average to zero. Of course, were this the case, we would expect all calculated interaction energies to be systematically renormalized by an error-dependent, fixed amount. Considering we have calculated many interaction energies to be approximately zero, we know that the systematic error is most likely negligible. Furthermore, we estimated  $E_{bu}$  in two ways: first, using Eqs. (3) and (4), and, second, using a single-atom, bulk supercell that contains neither adatoms nor a substrate. Because the two ways of calculating  $E_{bu}$  are so dissimilar, we can safely assume systematic error, if any exists, is different between the two. Because the two estimates agree remarkably well, the systematic error again is most likely negligible.

- 
- \* tjs@glue.umd.edu  
 † Corresponding author; einstein@umd.edu; http://www2.physics.umd.edu/~einstein/
- <sup>1</sup> L. D. Roelofs, in *Chemistry and Physics of Solid Surfaces, IV*, edited by R. Vanselow and R. Howe (Springer-Verlag, Berlin, 1982), 219; L. Österlund, M. Ø. Pedersen, I. Stensgaard, E. Lægsgaard, and F. Besenbacher, *Phys. Rev. Lett.* **83**, 4812 (1999).
  - <sup>2</sup> A. Bogicevic, S. Ovesson, P. Hyldgaard, B. I. Lundqvist, H. Brune, and D. R. Jennison, *Phys. Rev. Lett.* **85**, 1910 (2000).
  - <sup>3</sup> J.-S. McEwen, S. H. Payne, and C. Stampfl, *Chem. Phys. Lett.* **361**, 317 (2002); C. Stampfl, *Catalysis Today* **105**, 17 (2005); M. Borg, C. Stampfl, A. Mikkelsen, J. Gustafson, E. Lundgren, M. Scheffler, and J. N. Andersen, *ChemPhysChem.* **6**, 1923 (2005).
  - <sup>4</sup> W. Luo and K. A. Fichthorn, *Phys. Rev. B* **72**, 115433 (2005).
  - <sup>5</sup> A. P. J. Jansen and W. K. Offermans, *Lec. Notes Comp. Sci.* **3480**, 1020 (2005).
  - <sup>6</sup> G. Kresse and J. Hafner, *Phys. Rev. B* **47**, R558 (1993); *ibid.* **49**, 14251 (1994); G. Kresse and J. Furthmüller, *Comput. Mater. Sci.* **6**, 15 (1996); *Phys. Rev. B* **54**, 11169 (1996).
  - <sup>7</sup> T. L. Einstein, *Langmuir* **7**, 2520 (1991); G. Ehrlich and F. Watanabe, *ibid.* 2555; B.N.J. Persson, *Surf. Sci. Repts.* **15**, 1 (1992).
  - <sup>8</sup> T. L. Einstein, in: *Handbook of Surface Science*, edited by W. N. Unertl, Vol. 1 (Elsevier Science B.V., Amsterdam, 1996), ch. 11.
  - <sup>9</sup> H.-C. Jeong and E. D. Williams, *Surf. Sci. Rept.* **34**, 171 (1999).
  - <sup>10</sup> T. J. Stasevich, T. L. Einstein, R. K. P. Zia, M. Giesen, H. Ibach, and F. Szalma, *Phys. Rev. B* **70**, 245404 (2004).
  - <sup>11</sup> T. J. Stasevich, H. Gebremariam, T. L. Einstein, M. Giesen, C. Steimer, and H. Ibach, *Phys. Rev. B* **71**, 245414 (2005) [cond-mat/0412002].
  - <sup>12</sup> P. Hohenberg and W. Kohn, *Phys. Rev.* **136**, B864 (1964).
  - <sup>13</sup> W. Kohn and L. J. Sham, *Phys. Rev.* **140**, A1133 (1965).
  - <sup>14</sup> J.P. Perdew, in *Electronic Structure Theory of Solids*, edited by P. Ziesche and H. Eschrig (Akademie Verlag, Berlin, 1991); J.P. Perdew, J.A. Chevary, S.H. Vosko, K.A. Jackson, M.R. Pederson, D.J. Singh, and C. Fiolhais, *Phys. Rev. B* **46**, 6671 (1992).
  - <sup>15</sup> M. Methfessel and A. T. Paxton, *Phys. Rev. B* **40**, 3616 (1989).
  - <sup>16</sup> J. Neugebauer and M. Scheffler, *Phys. Rev. B* **46**, 16 067 (1992).
  - <sup>17</sup> K. A. Fichthorn and M. Scheffler, *Phys. Rev. Lett.* **84**, 5371 (2000).
  - <sup>18</sup> K. A. Fichthorn, M. L. Merrick, and M. Scheffler, *Phys. Rev. B* **68**, 041404(R) (2003).
  - <sup>19</sup> This behavior is in contrast, for example, to semiempirical studies of a few kinds of adsorbates on Pt(001), where sizable differences existed between chain and compact clusters, due seemingly to substantial configuration-dependent lateral relaxations; see A. F. Wright, M. S. Daw, and C. Y. Fong, *Phys. Rev. B* **42**, 9409 (1990).
  - <sup>20</sup> C. Fiolhais, L. M. Almeida, and C. Henriques, *Prog. Surf. Sci.* **74**, 209 (2003).
  - <sup>21</sup> D. Spišák, *Surf. Sci.* **489**, 151 (2001).
  - <sup>22</sup> X. Wang, Y. Jia, Q. Yao, F. Wang, J. Ma, and X. Hu, *Surf. Sci.* **551**, 179 (2004).
  - <sup>23</sup> H. S. Johnston and C. A. Parr, *J. Am. Chem. Soc.* **85**, 2544 (1963).
  - <sup>24</sup> N. A. Levanov, A. A. Katsnel'son, A. É. Moroz, V. S. Stepanyuk, W. Hergert, and K. Kokko, *Phys. Solid State* **41**, 1216 (1999).
  - <sup>25</sup> P. J. Feibelman, *Phys. Rev. B* **60**, 11 118 (1999).
  - <sup>26</sup> M.-C. Marinica, C. Barreteau, M.-C. Desjonquères, and D. Spanjaard, *Phys. Rev. B* **70**, 075415 (2004).
  - <sup>27</sup> R. C. Nelson, T. L. Einstein, S. V. Khare, and P. J. Rous, *Surf. Sci.* **295**, 462 (1993).
  - <sup>28</sup> M. Giesen, *Prog. Surf. Sci.* **68**, 1 (2001).
  - <sup>29</sup> R. Sathiyarayanan, T. J. Stasevich, and T. L. Einstein, unpublished.
  - <sup>30</sup> G. Boisvert, L. J. Lewis, and M. Scheffler, *Phys. Rev. B* **57**, 1881 (1998).